Chemical Engineering Journal 514 (2025) 163302

Contents lists available at ScienceDirect

Chemical Engineering Journal

journal homepage: www.elsevier.com/locate/cej

Amplified lung cancer hazards from surface defects in aged polypropylene microplastics

Yoojin Lee [a], Sung-eun Heo [a], Kyungtae Park [a], Hyungseok Yong [a], Yongho Lee [a], Taihyun Kim [a], Yoonsung Noh [a], Woojin Choi [a], Bumgyu Choi [a], Dahae Kim [b], Chae-Won Moon [b], Sang-Jun Ha [b], Jinkee Hong [a,*]

[a] Department of Chemical & Biomolecular Engineering, College of Engineering, Yonsei University, 50 Yonsei-ro, Seodaemun-gu, Seoul 03722, Republic of Korea
[b] Department of Biochemistry, College of Life Science & Biotechnology, Yonsei University, 50 Yonsei-ro, Seodaemun-gu, Seoul 03722, Republic of Korea

ARTICLE INFO

Keywords:
Microplastics
Polypropylene
Surface defect
Lung cancer
Proliferation

ABSTRACT

Microplastics, ubiquitous in the human body, often undergo an aging process due to long-term exposure to indoor and outdoor environmental conditions. While recent attention has focused on the impact of microplastics on cancer proliferation and metastasis in mouse cancer models, the specific properties of microplastics that influence cancer growth remain poorly understood. In this study, we compared and analyzed cancer cell proliferation based on the characteristics of aged polypropylene microplastics (PP MPs). Our findings reveal that aging microplastics not only increased and expedited cancer cell proliferation but also induced tumorigenic behavior in immune cells. Furthermore, microplastics exposed to the environment for extended periods were found to contribute to cancer metastasis. We propose that microplastics with prolonged environmental exposure can have significant adverse effects on patients with cancer, affecting both cancer and immune cells.

1. Introduction

Cancer patients typically spend their days either resting in a hospital ward or undergoing long-term surgery in the operating room, spanning from a few months to several years of treatment. A preliminary study indicated that there were approximately 1,924 ± 3,105 m^{-2} day^{-1} of microplastics in the operating room. The dominant types of microplastics in the operating room are the fragment shapes of polyethylene terephthalate (PET) and polypropylene (PP) [1]. In addition, the quantity of microplastics notably increases during surgery. Furthermore, a comparison of exposure levels between indoor and outdoor microplastics revealed that indoor environments harbor approximately 10 times more microplastics than outdoor settings. Consequently, cancer patients undergoing prolonged hospital stays, whether indoors or outdoors, are predicted to experience a more pronounced microplastic exposure than healthy individuals.

Microplastics pose a global concern not only for the environment but also for human health. Among the various diseases that microplastics can induce in the human body, cancer stands out as one of the most fatal. Interestingly, recent studies have highlighted the impact of microplastics can on the prognosis of cancer patients. For instance, PP microplastics have been implicated in the promotion of breast cancer metastasis [2]. Furthermore, polystyrene (PS) nanoplastics have been demonstrated to induce proliferation and metastasis in gastric cancer, as well as contribute to drug resistance in chemotherapy and immunotherapy [3]. In addition, polyethylene (PE) microplastics have been found to induce the proliferation of skin cancer cells, while having no effect on normal skin [4]. In conclusion, it is evident from both in vitro and in vivo studies that the influence of microplastics on cancer cells is significant.

Internalization of microplastics into the human body primarily occurs through ingestion and inhalation. Microplastics exposed to the body through ingestion can be readily excreted through urine, potentially resulting in fewer side effects [5]. However, microplastics that enter the lungs through inhalation are challenging to excrete from the body. Despite this challenge, minimal research has been conducted on the impact of microplastics on the internal environment of lung cancer cells, particularly regarding the characteristics of microplastics.

* Corresponding author.
E-mail addresses: carly6674@gmail.com (Y. Lee), heosungeun@yonsei.ac.kr (S.-e. Heo), ktpark.yonsei@gmail.com (K. Park), y940328@gmail.com (H. Yong), eyh1101@yonsei.ac.kr (Y. Lee), taihyunkim109@gmail.com (T. Kim), nohyoons1@gmail.com (Y. Noh), choiwoojin0321@gmail.com (W. Choi), xpo95son@gmail.com (B. Choi), dlqnsl6297@naver.com (D. Kim), moon3277@naver.com (C.-W. Moon), sjha@yonsei.ac.kr (S.-J. Ha), jinkee.hong@yonsei.ac.kr (J. Hong).

https://doi.org/10.1016/j.cej.2025.163302
Received 26 May 2024; Received in revised form 29 April 2025; Accepted 30 April 2025
Available online 1 May 2025

In this study, we examined the long-term exposure of cancer cells to environmentally exposed fragmented microplastics and assessed the resulting prognosis for patients with cancer based on the characteristics of the microplastics (Fig. 1). Given that PP microplastics are the prominent polymer type in human lungs at the concentration of 2–3 MP/g of lung tissue [6,7], we subjected PP microplastics to aging process to simulate environmental exposure at indoors and outdoors ranging from 0 to 3 years. We hypothesized that as the microplastics aged, changes in their size and surface properties would occur, with these two factors having the greatest impact on cancer cells. In addition, we propose that microplastics function as carriers, facilitating the delivery of the Notch-1 transmembrane receptor protein from one cancer cell to adjacent cells, thereby enhancing communication between cancer cells and expediting the development of a tumorigenic environment.

2. Results

2.1. Characterization of long-term environmentally exposed microplastics

Based on our previously developed technology for mimicking long-term natural environment exposure [8], we fragmented and aged PP plastics to simulate 0, 1, 2, and 3 years of environmentally exposed microplastics (Fig. 2a). Over time, the color of the PP microplastics gradually transitioned toward yellow (Supplementary Fig. 1). The morphology of the PP microplastics was assessed by using field emission scanning electron microscopy (Fe-SEM), and their sizes were measured using ImageJ. As displayed in Fig. 2b and Supplementary Fig. 2, fragmented microplastics exhibited a random shape with sharp edges and a rough surface. Before aging, microplastics exhibited a diverse size distribution ranging from 0 to 20 μm, but with aging, the distribution narrowed to sizes below 10 μm (Supplementary Fig. 3). Specifically, the size of the PP microplastics significantly decreased from 8.41 μm to 4.08 μm, 3.75 μm, and 3.54 μm after 1, 2, and 3 years of aging, respectively (Fig. 2c). We further hypothesized that the reduction in PP microplastic size after aging is attributable to both physical and chemical alterations. To determine which characteristic underwent a more dominant change, we conducted additional physicochemical property analysis. Despite the aging process, the peak of PP microplastics consistently appeared at 2800–3000 cm^{-1} (CH stretching vibrations) without any Raman shift in the Raman spectrum (Supplementary Fig. 4). However, the peaks of the CH stretching vibrations exhibited a relative weakening corresponding to the aging duration of the PP microplastics (Fig. 2d). Previous studies have reported significant changes in the Raman spectrum after the aging of microplastics [9]. In addition, the Raman spectrum is closely related to the size and surface roughness of the particles [10]. As the particle sizes decrease and the surface roughness increases, the intensity of the Raman spectrum decreases. This phenomenon occurs because the Raman signal can be detected in multiple areas due to spatial distribution, resulting in a reduced amount of light collected and detected by Raman spectroscopy [11,12]. Given that the area of Raman intensity notably decreased especially after 3 years of aging (Supplementary Fig. 5), we confirmed the alterations in physical properties such as size reduction and surface defects of PP microplastics through Raman spectroscopy after aging, in addition to Fe-SEM. In addition, atomic force microscopy (AFM) results showed that the surface roughness of PP microplastics increased with aging time (Fig. 2e, Supplementary Fig. 6). To further confirm the surface defects of the microplastics, we performed BET analysis to examine changes in the surface area of the microplastics resulting from the aging process (Fig. 2f). The analysis revealed that microplastics aged for 0, 1, 2, and 3 years exhibited surface areas of 3.02, 3.59, 8.40, and 8.68 m^2/g, respectively. This indicates a gradual increase in surface area with aging time. These observed

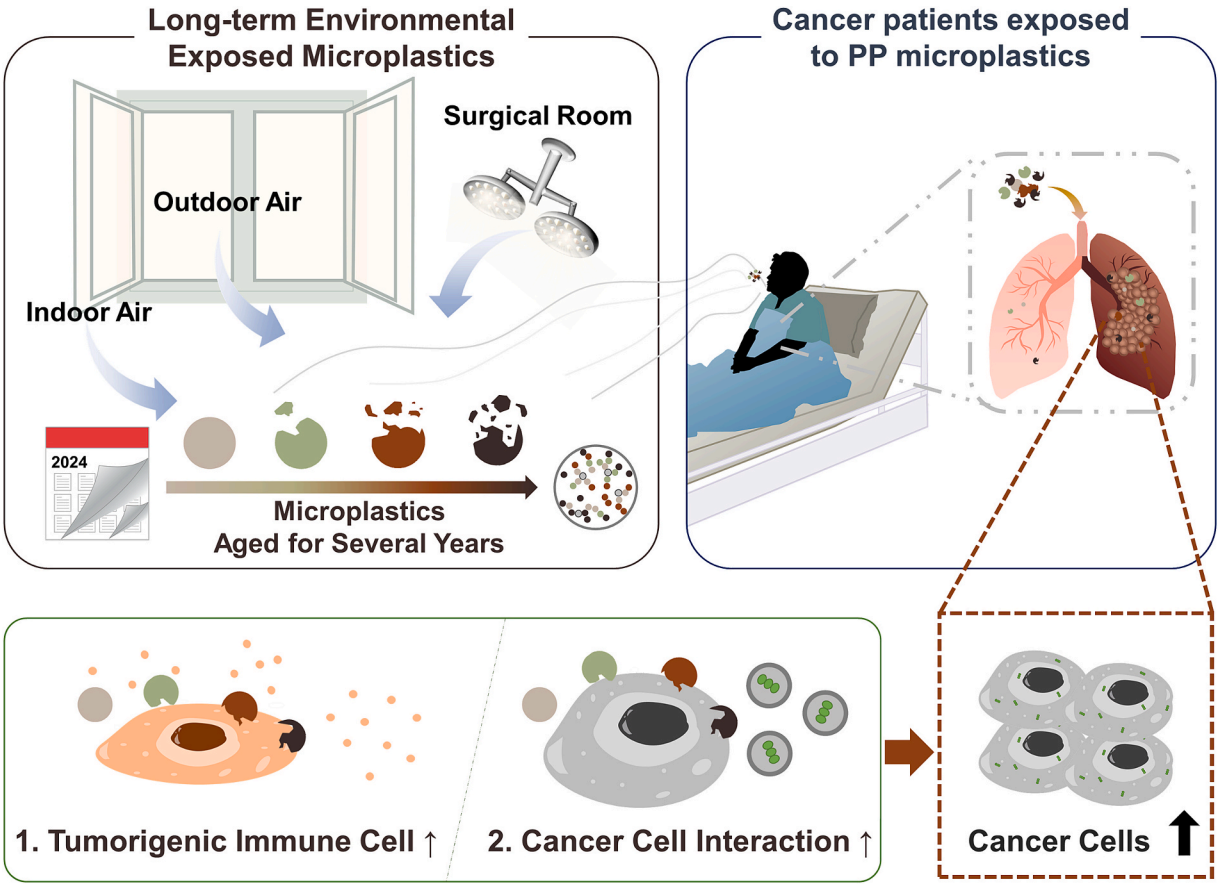

Fig. 1. Schematic of the proliferation of non-small cell lung cancer cells in patients with cancer accelerated by environmentally exposed microplastics.

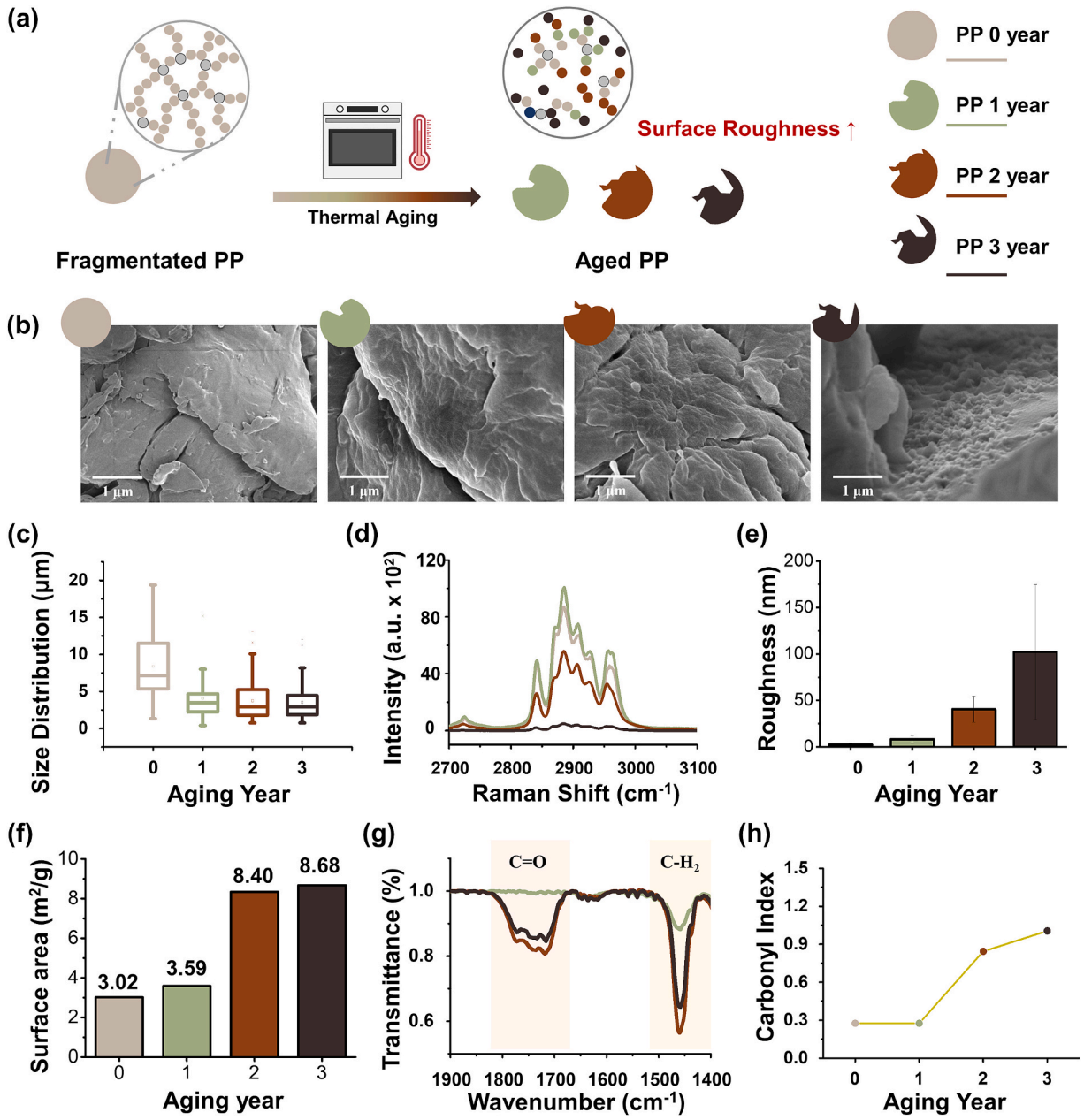

Fig. 2. Polypropylene microplastics characterization according to the aging time. (a) Illustrated polymer chain deformation in microplastics during the aging process. (b) SEM imaging of polypropylene (PP) microplastics (0, 1, 2, and 3 years). Scale bars: 1 μm. (c) Size distribution of PP microplastics according to the SEM images. (d) Raman spectra of PP microplastics. (e) Average surface roughness measured by AFM. (f) Surface area of aged PP microplastics determined by BET. (g) ATR-FTIR of PP microplastics. (h) Carbonyl index (Area of C═O / Area of CH2 scissoring peak) increased with aging time according to ATR-FTIR.

physical property changes collectively indicate that the aging process induced surface defects on microplastics, which are attributable to the increase in surface roughness leading to an increase in surface area.

After identifying the physical changes, we conducted FT-IR, TGA, and DSC analyses to validate the chemical alterations. Fourier-transform infrared spectroscopy (FT-IR) showed the emergence of new peaks corresponding to carbonyl groups (C═O) within the range of 1600–1900 cm^{-1} after the aging of PP microplastics (Fig. 2g, Supplementary Fig. 7). Based on the FT-IR results, we calculated the carbonyl index (CI) and compared the values to evaluate changes over aging time (Fig. 2h). The analysis indicated an increase in the carbonyl index of PP microplastics with aging, indicating oxidation during the aging process. Notably, there was no significant oxidation observed in PP microplastics aged for 1 year. However, in the second year, a steep slope indicated rapid oxidation, whereas a gentler slope compared with the 2-year-aged sample was observed in the PP microplastics aged for 3 years, consistent with the BET results. Furthermore, based on the TGA and DSC results (Supplementary Fig. 8), the degradation of PP microplastics significantly increased after aging. The maximum degradation temperature (Tmax) of the PP microplastics ranged from 400 to 480 °C, with an increase in the decomposition temperature observed after aging. This indicates the formation of stable polymers resulting from chemical bond rearrangements and various chain scissions within the polymer [13,14]. In addition, a mass change position between 0 and 300 °C, indicating high oxidation induced by unstable intermediates such as C═O [15], consistent with FT-IR. In summary, PP microplastics undergo rapid initial degradation after aging, leading to decreased thermal stability. However, there was a lack of correlation between aging years and changes in thermal stability, indicating that the tendency of chemical property changes was not as distinct as changes in physical properties. In

conclusion, we found that the physical properties of PP microplastics have a greater impact after aging than their chemical properties.

2.2. Aged PP microplastics induce tumorigenicity in immune cells

Next, we exposed both aged and un-aged PP microplastics to RAW 264.7 macrophage cells to explore the *in vitro* adverse effects of microplastics on immune cells based on aging time. First, we evaluated the toxicity of PP microplastics on RAW 264.7 cells using flow cytometry, which revealed an approximately 10 % decrease in viability attributed to PP microplastics (Fig. 3a). Although toxicity slightly increased with longer aging periods, with all survival rates remaining above 80 %, the cytotoxicity caused by PP microplastics was deemed insignificant. Furthermore, the impact on viability was assessed using the CCK-8 Assay, which also exhibited negligible effects and supported the cytotoxicity results (Supplementary Fig. 9). Despite the absence of a significant cytotoxic effect of microplastics on macrophage cells, microscopic examination from various angles revealed elongation in the morphology of RAW 264.7 cells following treatment with both aged and un-aged PP microplastics (Fig. 3b, Supplementary Fig. 10), indicating the polarization of macrophages toward M2. Ultimately, we performed flow cytometry analysis to evaluate the degree of polarization with the M2 surface marker CD206 and the M1 surface marker CD80 (Fig. 3c-d, Supplementary Figs. 11,12). The results revealed an increase in the expression of the CD206 marker after treatment with 0-, 1-, 2-, and 3-years aged PP microplastics, with percentages of 1.24 %, 2.91 %, 10.8 %, and 17.2 %, respectively. Although there was also a slight increase in M1 polarization, unlike M2, it indicated negligible polarization levels, the levels remained negligible compared with M2 polarization, with the values of 0.05 %, 0.17 %, 0.21 %, and 0.37 %, all below 0.5 %. In conclusion, comparing the expression of CD80 and CD206, it is evident that CD206 expression exhibited a higher increase with aging

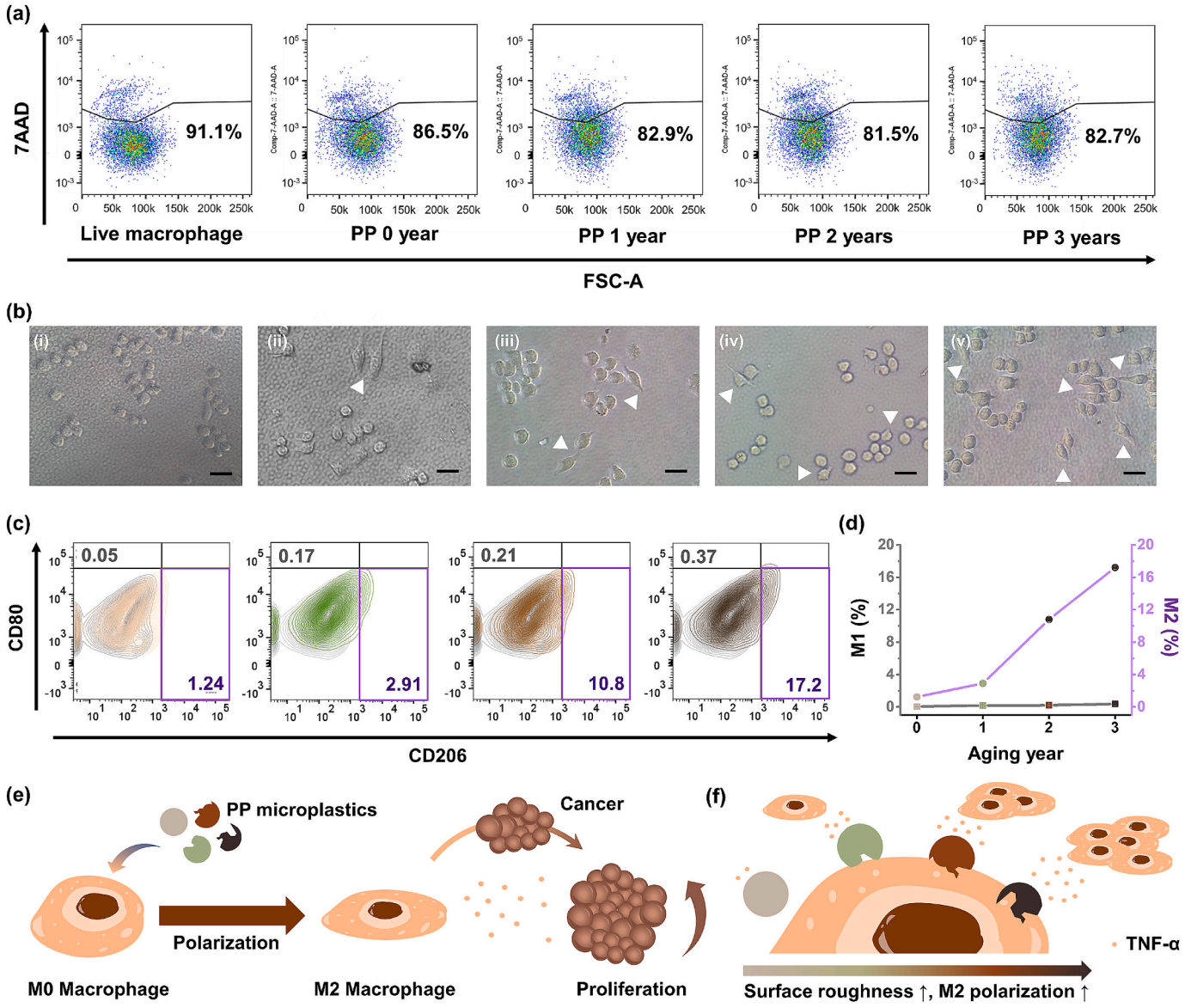

Fig. 3. Polypropylene microplastics induced M2 polarization in macrophage. a Cell viability with polypropylene (PP) microplastics at 100 μg/mL, 10 μg/mL and 1 μg/mL was measured by flow cytometry after 7 days of exposure. b Morphologies of RAW 264.7 cells observed by microscopic images. ((i) Untreated cells, and cells treated with (ii) 0 year of PP aging, (iii) 1 year of PP aging, (iv) 2 years of PP aging, and (v) 3 years of PP aging. Scale bar: 20 μm. c Comparison of M1 and M2 polarization after the treatment of PP microplastics by flow cytometry. d M2 polarization (CD206 marker) increment occurred by aged microplastics. e RAW 264.7 macrophage cell line treated with PP microplastics induced M2 polarization, which may further lead to cancer proliferation. f Mechanism of aged PP microplastics inducing M2 polarization of macrophages.

time than CD80 (Fig. 3d). Therefore, it can be concluded that M0 RAW 264.7 macrophages undergo distinct polarization toward M2 rather than M1. M2 polarization of macrophages contributes to tumor proliferation [16] (Fig. 3e). Hence, it indicates that immune cells could promote tumor proliferation after exposure to PP microplastics, especially those aged over the long term. We then sought to analyze the effects of PP microplastics on other immune cells besides macrophages, by treating aged and un-aged PP microplastics with mice dendritic cells and exposing these cells to T cells (Supplementary Fig. 13). Consequently, FSC-A, which represents the viability of T cells, slightly decreased with aging time, indicating that the remaining PP microplastics attached to dendritic cells after exposure had an impact on the T cell viability. In particular, after exposure to aged PP microplastics, the cytokine level of TNF-α and IFNγ significantly increased. This indicates the potential of T cells to induce inflammation after encountering dendritic cells that have processed microplastics.

The previous studies reported that microplastics induce M1 polarization in macrophages but not M2 polarization [17–19]. However, our studies showed opposite results. We attribute this difference to surface characteristics, while previous studies used polystyrene microplastics with smooth surfaces, which may affect M1 polarization differently. In contrast, aged PP microplastics exhibited surface defects (Fig. 2b-e), which can further increase the TNF-α expression due to higher cell adhesion ability resulting from increased surface roughness [20,21]. This could lead to M2 polarization (Fig. 3f), which is consistent with the results of Supplementary Fig. 13. Thus, we concluded that fragmented and aged microplastics may favor M2 polarization rather than M1 polarization, leading to the generation of tumorigenic immune cells that can further increase the risk of cancer proliferation.

2.3. Lung cancer cell proliferation induced by aged PP microplastics

Microplastics pose a long-term risk because of their potential to reside in the body for extended periods, given the possibility of continuous exposure in daily life [22]. However, most of the studies related to microplastics have focused on short-term *in vitro* tests [23]. Therefore, to assess the long-term proliferation of non-small cell lung cancer cell lines according to the aging years of PP microplastics, we used two different cell line of A549 proliferative cells and NCI-H1650 smoker lung cancer cells, and treated 100, 10, and 1 μg/mL of aged and un-aged PP microplastics for 7 days (Fig. 4a). The results showed that the addition of 100 μg/mL PP microplastics increased the proliferation of A549 lung cancer cells (Fig. 4b). In particular, after long-term exposure of 7 days, 3-year-aged PP microplastics exhibited approximately twice the proliferation rates compared with untreated cells (Supplementary Fig. 14, 16). Similar results were also observed at concentrations of 10 (Fig. 4c) and 1 μg/mL (Fig. 4d), respectively, indicating a decrease in proliferation as the concentration of PP

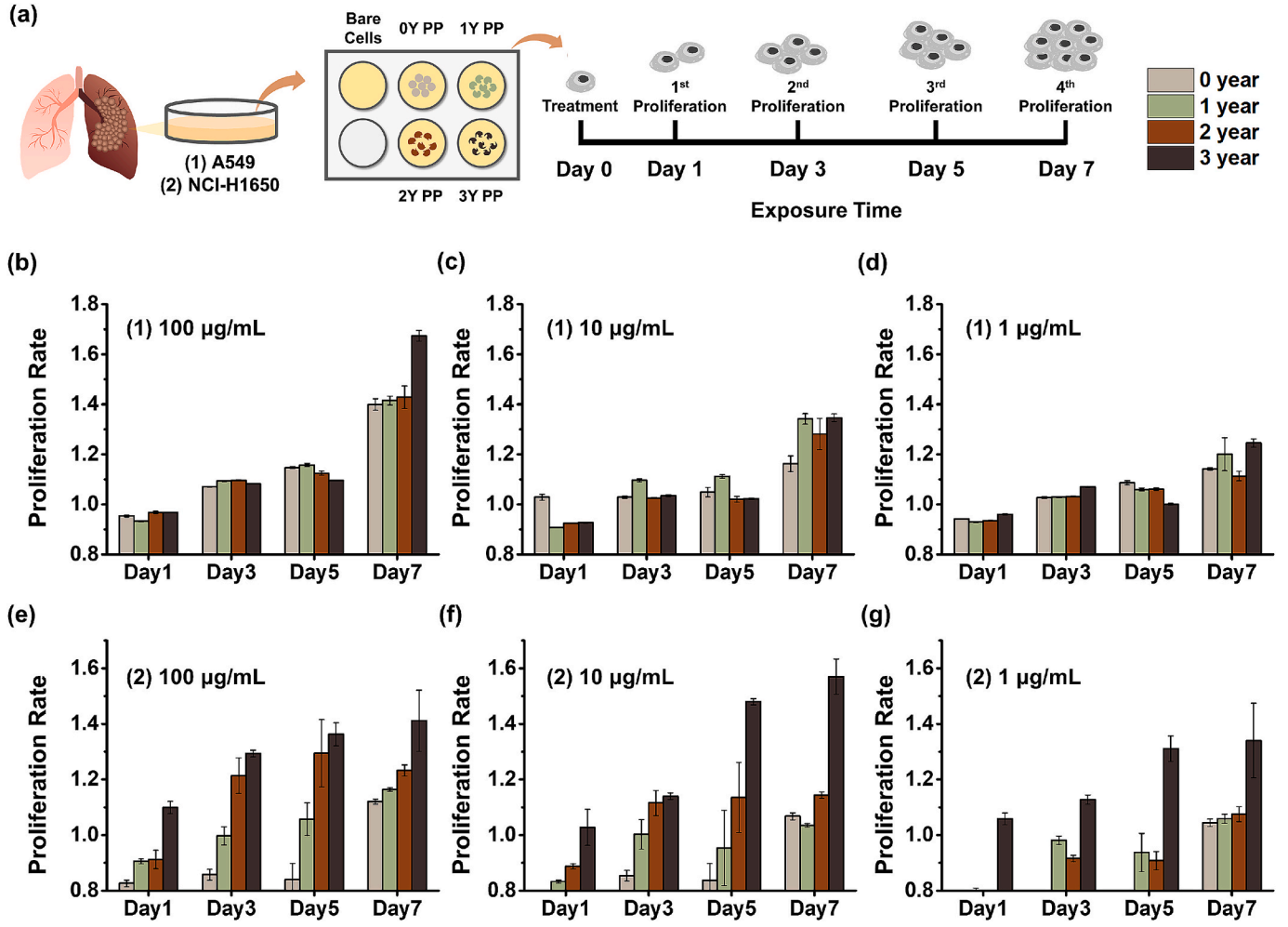

Fig. 4. The proliferation rate of A549 non-small cell lung cancer cell was increased by long-term exposure to aged polypropylene (PP) microplastics. (a) A schematic of long-term in vitro A549 and NCI-H1650 non-small cell lung cancer cell proliferation test. A549 proliferation rate based on the date of cellular exposure to (b) 100 μg/mL, (c) 10 μg/mL, and (d) 1 μg/mL of PP microplastics. NCI-H1650 proliferation rate based on the date of cellular exposure to (e) 100 μg/mL, (f) 10 μg/mL, and g 1 μg/mL of PP microplastics.

microplastics decreased. The effect of PP microplastics on NCI-H1650cells also revealed that the 100 μg/mL PP microplastics with fewer aging years did not show significant proliferation compared with untreated NCI-H1650 (Fig. 4e), whereas PP microplastics aged for 3 years induced approximately twice the proliferation rates at day 7 (Supplementary Fig. 15, 17), similar to A549. In particular, in contrast to A549, NCI-H1650 exhibited high proliferation even at concentrations of 10 μg/mL (Fig. 4f) and 1 μg/mL (Fig. 4g) in the 3-year-aged samples. Moreover, both A549 and NCI-H1650 cells exhibited significant proliferation upon treatment with 3-year-aged PP microplastics, particularly after long-term exposure, confirming that aged PP microplastics greatly induce cancer cell proliferation (Supplementary Fig. 16-17). Moreover, treatment with aged PP microplastics at concentrations of 0.5 μg/mL and 0.1 μg/mL similarly led to a significant increase in the proliferation of A549 and NCI-H1650 cells (Supplementary Fig. 18). Notably, PP microplastics aged for 3 years had a pronounced effect on cancer cell proliferation even at low concentrations. In conclusion, we have demonstrated that PP microplastics promote the proliferation of non-small cell lung cancer cells depending on the aging year, and NCI-H1650 smoker lung cancer cells exhibit greater sensitivity compared

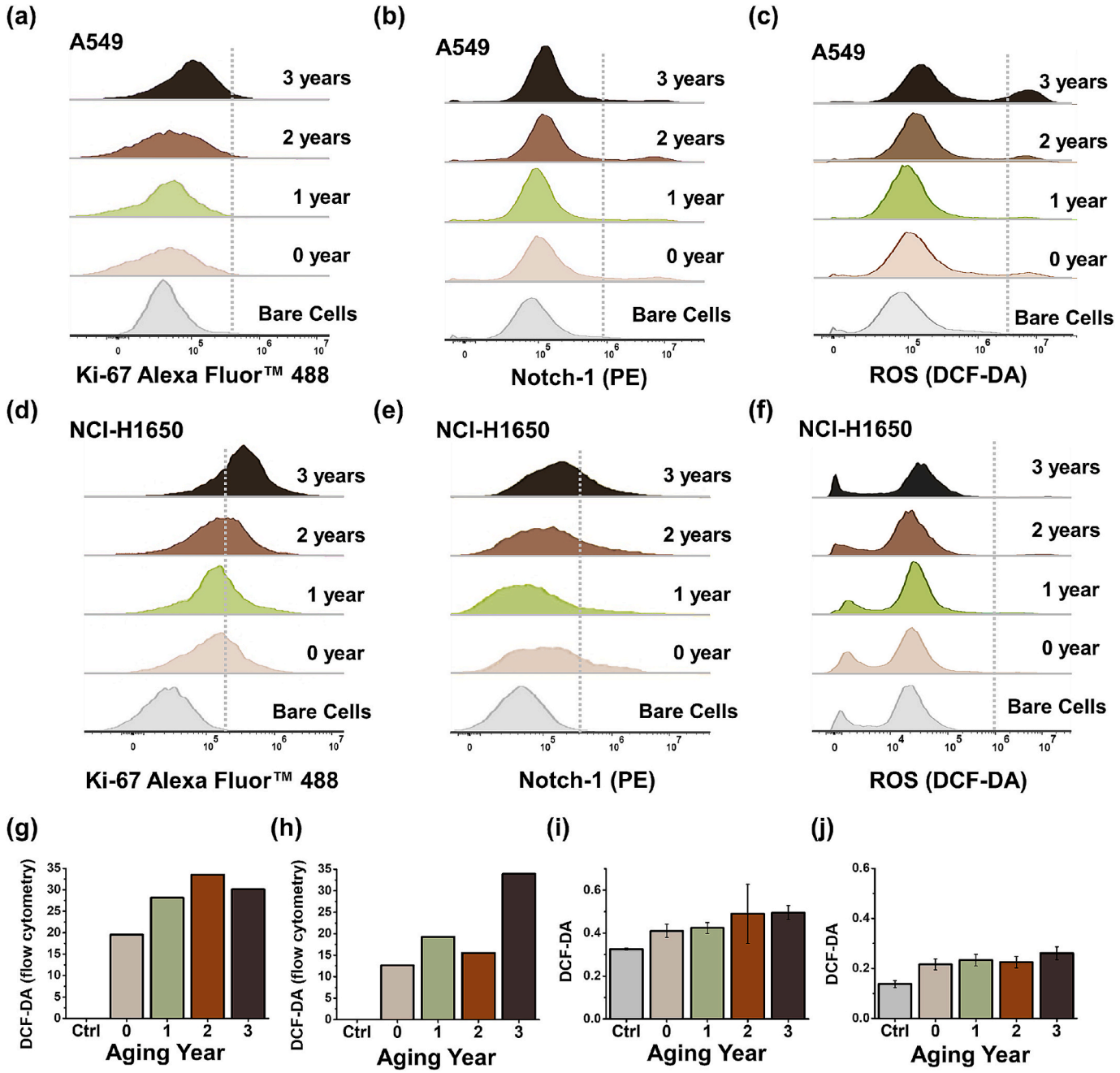

Fig. 5. Proliferation and drug resistance (Ki-67), elongation and metastasis (Notch-1) and ROS (DCF-DA) markers determined by flow cytometry in A549 and NCI-H1650 cells. (a) Ki-67 markers, (b) Notch-1 markers, (c) DCF-DA compared between untreated A549 cells and A549 cells exposed to 0-, 1-, 2-, 3-year-aged polypropylene (PP) microplastics. (d) Ki-67 markers, (e) Noth-1 markers, (f) DCF-DA compared between untreated NCI-H1650 cells and NCI-H1650 cells exposed to 0-, 1-, 2-, 3-year-aged polypropylene (PP) microplastics. DCF-DA of (g) A 549, and (h) NCI-H1650 determined by flow cytometry, and DCF-DA of (i) A549 and (j) NCI-H1650 measured by microplate reader.

with A549 cells.

2.4. Ki-67 and Notch-1 markers in relation to PP microplastics aging time

To analyze the mechanism of lung cancer cell proliferations induced by PP microplastics based on the aging years, we exposed A549 and NCI-H1650 lung cancer cells to 100 μg/mL of aged and un-aged PP microplastics 7 days *in vitro* and examined the expression level of Ki-67. As shown in Fig. 5a and 5d, Ki-67 expression in A549 and NCI-H1650 cells significantly increased with the aging of PP microplastics. However, NCI-H1650 cells exhibited greater proliferation compared to A549 cells, which is consistent with the findings in Fig. 4b-g. Moreover, considering that Ki-67 expression is associated with drug resistance [24], these results indicate that PP microplastics induce drug resistance in lung cancer cells based on the aging year, with NCI-H1650 smoker lung cancer cells exhibiting higher drug resistance than A549 cells. Treatment with the representative chemotherapy drug cisplatin showed that aged PP microplastics diminished its anticancer efficacy by reducing cell death in A549 and NCI-H1650 cells. Drug resistance was further enhanced with increasing microplastic aging (Supplementary Fig. 19). In addition to the proliferation rate (Fig. 4), NCI-H1650 cells exhibited noticeable elongation in morphology after treatment with aged and un-aged PP microplastics (Supplementary Fig. 15). Cancer cell elongation is a factor that can induce metastasis [25–27]. Hence, to confirm the potential of aged PP microplastics to induce elongation and metastasis of lung cancer cells, we conjugated Notch-1 antibodies and conducted flow cytometry analysis. NCI-H1650 cells exhibited a significantly increased expression of Notch-1 signals based on aging time (Fig. 5e), whereas A549 had a lesser effect (Fig. 5b), which was consistent with the result of Ki-67 expression and the morphology of A549 (Supplementary Fig. 14) and NCI-H1650 cells (Supplementary Fig. 15).

During the elongation of cancer cells, the cell cycle initiates with the G1 phase, which represents cell growth [28]. An increase in reactive oxygen species (ROS) levels promotes the G1 phase of the cell cycle [29]. Therefore, as ROS increases, cancer cells proliferate. We analyzed ROS generation in A549 and NCI-H1650 cells induced by aging PP microplastics using DCF-DA staining. As a result, 0-, 1-, 2-, and 3-year-aged PP microplastics induced ROS increases of 19.5 %, 28.1 %, 33.5 %, and 30.1 %, respectively in A549 cells (Fig. 5c, g) and 12.6 %, 19.3 %, 15.5 %, and 33.9 %, respectively in NCI-H1650 cells (Fig. 5f, h). These findings indicate that PP microplastics clearly increased ROS levels in lung cancer cell lines depending on the aging time. Intracellular ROS levels measured by DCF-DA assay using a fluorescence microplate reader also showed consistent results with flow cytometry, with increases of 1.26, 1.30, 1.51, and 1.52-fold in A549 cells (Fig. 5i), and 1.57, 1.69, 1.64, and 1.89-fold in NCI-H1650 cells (Fig. 5j).

3. Discussion

Microplastics have recently garnered global attention as hazardous substances with most studies focusing on their environmental impact, while their effects on human health remain largely uncertain. However, recent research indicates that micro- and nanoplastics may possess carcinogenic potential [30], potentially affecting human cells and tissues at a cellular level. Consequently, investigations into the impact of microplastics on various cell types, including iPSCs [31], red blood cells, and human dermal fibroblasts [32], have been undertaken. Despite indications on the potential carcinogenicity of microplastics, research on their effects specifically on cancer cells remains limited. It is hypothesized that if microplastics could affect healthy individuals, the ramifications for cancer patients would be substantial. Therefore, by simulating environmental exposure changes through the aging of commercially widely used PP microplastics and treating them with lung cancer cells, we confirmed that the aging of microplastics over time induces an increase in ROS levels in cancer cells, thereby promoting proliferation and metastasis.

We analyzed the above phenomena considering the characteristics of microplastics, which have not been previously studied. In particular, we selected polypropylene (PP) for this study because its brittle and fragile nature makes it more prone to degradation compared to other common microplastics such as polystyrene (PS) and polyethylene (PE) [33]. These properties make PP especially suitable for clearly demonstrating the dramatic effects of microplastic aging. First, we aged PP microplastics annually to analyze their physical (size and surface) and chemical (functional groups and thermal stability) characteristics according to the aging process. Our goal was to investigate the characteristics that have the greatest impact on cancer cells. Thermodynamic properties did not significantly emphasize the effects of aging (Supplementary Fig. 7). However, we validated an increase in the carbonyl index using FT-IR (Fig. 2h), which indicates the oxidation of microplastics during the aging process. The increase in the carbonyl index was less pronounced between periods of 2–3 years compared with the rapid rise observed from 1 to 2 years. However, contrary to this trend, PP microplastics aged for the longest duration (3 years) induced sudden proliferation on the 7th day in both A549 and NCI-H1650 cell lines (Fig. 4), which is inconsistent with chemical properties changes. In contrast, regarding physical properties, there was no significant difference between 0 and 1 year, but clear aging effects were evident when progressing from 1 to 2 years, particularly with noticeable surface changes when aging from 2 to 3 years (Fig. 2f-g). These results were consistent with the increase in ROS levels, proliferation, and metastasis of cancer cells (Figs. 4-5). The rough surface characteristics of microplastics can enhance their attachment to cells, thereby triggering early cellular responses [34,35]. Subsequently, the increased carbonyl index promotes redox reactions, facilitating electron transfer and leading to elevated ROS production [36,37]. We measured the washed PP microplastics during the proliferation test. As a result, approximately 20–30 % of PP microplastics aged for 0 and 1 year were washed out during the process, whereas 2- and 3-year-aged PP microplastics remained well attached to the cells without being washed away (Supplementary Fig. 20-21). These results not only indicate that PP microplastics were not notably washed out during proliferation test, but also indirectly suggest that the adhesion of PP microplastics aged for 2–3 years was relatively strong and well maintained. Consequently, the aging of microplastics, through both physical and chemical property changes, may significantly contribute to the proliferation of lung cancer cells.

Our next step is to elucidate the specific pathways through which the physical characteristics of microplastics affect cancer cells. This is a particularly important task. The aging process introduces surface defects, leading to a significant increase in the surface roughness of the microplastics. The surface molecules and surface chemistry play a crucial role in determining the surface energy of a substrate, which in turn influences cell adhesion, growth, and proliferation [38]. Consequently, the higher surface roughness of microplastics may provide cancer cells with more opportunities to attach to the microplastics, potentially explaining their increased proliferation in response to aging-related surface changes of microplastics.

In addition to the proliferative marker Ki-67, the Notch-1 signaling analysis conducted in this study focused on communications between adjacent cells. Notably, the high expression of Notch-1 indicates that lung cancer cells engage in communication with distant cells. This interaction occurs via ligands from neighboring cells through soluble

molecules. Through Notch-1 signaling, nearby microenvironmental cells are educated, leading to pro-tumorigenic behavior [39,40]. Therefore, the Notch signaling pathway emerges as a critical mechanism that drives the proliferation and metastasis of lung cancer cells, as they can be released from lung cancer cells' exosomes and transferred to surrounding cancer cells [41]. Previous studies demonstrated that extracellular vesicles, such as exosomes, separated from the serum of pigs exposed to polyethylene terephthalate (PET) microplastics exhibit PET altered miRNA within the extracellular vesicles and could transport PET to neighboring cells [42].

In summary, the aging process of PP microplastics results in increased roughness due to surface defects, thereby increasing surface area and promoting contact between cells and microplastics (Fig. 6). These microplastics potentially serve as carriers for delivering Notch-1 signals to the surrounding lung cancer cells. Furthermore, given that NCI-H1650 exhibits higher expression of SIRT2 mRNA [43] than A549, which is associated with senescence [44] and tumorigenicity, NCI-H1650 may exhibit heightened sensitivity to microplastics compared with A549 (Figs. 4-5). Consequently, we posit that aged microplastics could substantially promote the proliferation and metastasis of lung cancer especially among smokers.

Aged PP microplastics are found to not only affect the proliferation of cancer cells, but also induce M2 macrophage polarization, which can further promote cancer. Relatively higher surface roughness (Ra $<$ 200 nm) induced M2 macrophage polarization, while smoother surfaces were not associated with M2 polarization [45]. Therefore, we speculate that the rough surface may be the reason for M2 polarization in macrophages.

In this study, we utilized additive-free polypropylene microplastics to isolate and clarify the carcinogenic effects specifically associated with the aging process of microplastics. While this approach allowed us to focus on the intrinsic physicochemical changes of aged microplastics, it is also well known that certain plastic additives can contribute to lung carcinogenesis [30] and may be more readily released following the aging process [46,47]. Therefore, in real-world scenarios, aged microplastics circulating within the human body could exert carcinogenic effects not only through aging-induced surface changes but also via the release of harmful additives. Further in vivo studies will be essential to validate these observations and to better understand their broader physiological relevance.

4. Methods

4.1. Polypropylene microplastics

Amorphous polypropylene (PP) pellets (#428175, Sigma) with18 mm in size were used for this study. Initially, their surfaces were washed with 70 % ethanol. After drying at room temperature, the pellets were placed into the white ball case of the ball mill (Fritsch, Idar-Oberstein, Germany) and securely sealed. Subsequently, the ball containing PP pellets was immersed in liquid nitrogen for 10 min to achieve freezing. After completely freezing the PP pellet, the ball was milled at 45 rpm for 2 min, followed by another 2 min immersion in liquid nitrogen for freezing. This process was repeated 10 times to ensure thorough fragmentation. After fragmentation, the ball-milled plastic fragments were collected using 100 % ethanol. The plastic fragments dispersed in 100 % ethanol were filtered sequentially through the 300, 100, and 20 μm pore sized standard sieve. PP microplastics size under 20 μm were collected in 100 mL glass vial and dried for 2 days at 45 °C in a vacuum oven.

4.2. Environmental exposure simulation by thermal accelerated aging

Thermal accelerated aging was conducted to simulate natural environment exposure [48].

$$\text{Accelerated Aging Time} = \frac{(365days) \times t_E}{\frac{Q_{10}}{10} \times (T_A - T_S)}$$

The calculation of accelerated aging time is stated above, where t_E represents the required time for simulating natural environment exposure, T_A denotes the accelerated aging temperature, T_S signifies the temperature of the surrounding environment during acceleration, Q_{10} represents the aging factor with a value of 2 [49].

4.3. Characterization of polypropylene microplastics

The surface morphology of PP microplastics at various aging durations was examined by field emission scanning electron microscope (FE-SEM, JSM- 7610F-Plus, JEOL), and particle size was measured by counting the PP microplastics in SEM images using ImageJ software. In addition, Raman spectroscopy (XploRATM PLUS, Horiba), differential scanning calorimetry (DSC25, TA Instruments), and thermogravimetric analysis (TGA, Q50, TA Instruments), atomic force microscopy (AFM,

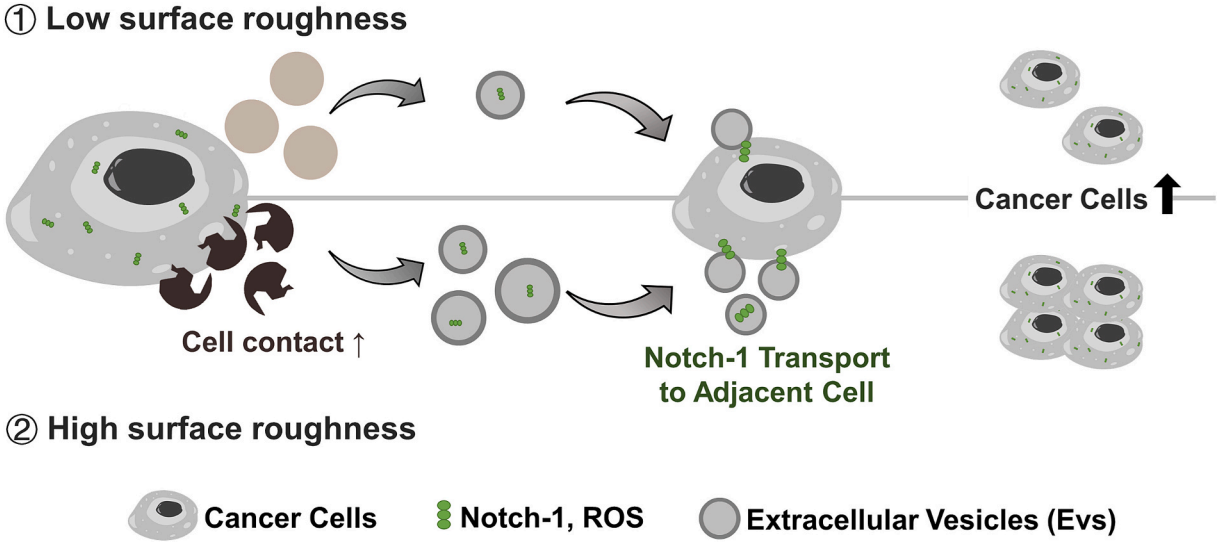

Fig. 6. Schematic of lung cancer cell proliferation induced by polypropylene microplastics.

NX-10; Park Systems, Suwon, Korea) were employed to characterization of aged PP microplastics. Nitrogen adsorption measurements of aged PP microplastics were performed using a Brunauer–Emmett–Teller (BET) analyzer (ASAP 2020 system, Micromeritics Instrument Corp., USA) to calculate the specific surface area (S_{BET}). Fourier transform infrared (FTIR) spectroscopy (VERTEX 70, Bruker) were performed to identify the chemical changes in the PP microplastics. The carbonyl index was calculated using the following formula:

$$\text{Carbonyl index (CI)} = \frac{\text{Absorbance (C = O peak from } 1,850 - 1,650\ \text{cm}^{-1})}{\text{Absorbance (CH}_2\text{ scissoring peak from } 1,500 - 1,420\ \text{cm}^{-1})}$$

4.4. RAW 264.7 macrophage cell culture and viability test

Murine macrophages (RAW264.7) were obtained from the Korean Cell Line Bank (Seoul, Korea). Cells were cultured in low glucose-Dulbecco's modified eagle medium (#11885084, Gibco, Grand Island, NY) supplemented with 10 % heat-inactivated fetal bovine serum (#S001-01, Welgene, Gyeongsan, Korea) and 1 % penicillin–streptomycin-glutamine (#10378016, Gibco). The morphology of Raw 264.7 cells was observed by microscopy. To investigate the viability against the samples, 15 000 cells per well were seeded in 12 well plates and 0-, 1-, 2-, and 3-year-aged PP microplastics were simultaneously loaded at concentration of 100, 10, and 1 μg/mL (n = 3). After 2 days of treatment, cells were washed with phosphate buffered saline (PBS, # 10010049, Gibco) and retreated with the same concentration of PP microplastics. The washing process was repeated 3 times during culture. After a total exposure period of 7 days, a cell counting kit-8 (CCK-8) reagent (#CCK-3000, Dongin Biotech Co., Korea) was introduced into the culture medium, and incubated for 1 h. Absorbance at a wavelength of 450 nm was measured using a plate reader (Spectra Max 340 PC; Molecular Devices, San Jose, CA, USA).

4.5. Assay of macrophage polarization using RAW 264.7 cells

Raw 264.7 cells (1×10^5 cells) were seeded into each well of a 6-well plates, treated with 100 μg/mL of 0-, 1-, 2-, and 3-year-aged PP microplastics, and cultured for 7 days. During culture, cells were washed with PBS. On day 7, flow cytometry analysis was conducted to quantify the populations of M1 and M2 macrophages using CD80 (M1 marker) and CD206 (M2 marker) cell surface markers. The cells were treated with CD16/32 for 20 min to block nonspecific binding. Subsequently, they were stained with FITC anti-mouse CD80, Alexa Fluor 647 anti-mouse CD206, PE anti-mouse F4/80, and PB anti-mouse/human CD11b for 30 min. The cells were then washed with FACS buffer three times. Finally, the 7-AAD staining solution was added and incubated for 30 min. The data were acquired using a BD FACSVerse system (BD Bioscience, CA, USA) and analyzed with FlowJo X software (Flowjo, LLC, Ashland, OR, USA).

4.6. Bone marrow-derived dendritic cells (BMDCs) differentiation

BMDCs were differentiated from bone marrow cells isolated from the femurs of naïve B6 mice (6–8 weeks). Red blood cells (RBCs) from the bone marrow were lysed using ACK lysis buffer (Gibco Laboratories). After RBC lysis, single-cell suspensions were cultured in RPMI (Corning) supplemented with 10 % FBS, 1 % penicillin/streptomycin, and 20 ng/mL recombinant murine GM-CSF (JW Creagene). Culture media were replenished on days 3 and 6. For maturation of BMDCs, 20 ng/mL LPS (Sigma Aldrich) was added to the culture media after 6 days. After 7 days of culture, nonadherent cells were collected and pelleted by centrifugation at 2,000 rpm for 5 min at room temperature.

4.7. In vitro evaluation of T cell activation by bone marrow-derived dendritic cells (BMDCs)

The BMDCs collected by centrifugation were resuspended in 1 × phosphate-buffered saline (PBS, pH 7.4), and divided into six 10^6 cells in 1 mL of PBS. These cells were centrifuged at 2,000 rpm for 5 min at room temperature, and treated with 100 μg/mL of 0-, 1-, 2-, and 3-year-aged PP microplastics, which were well dispersed in 1 mL of culture media each. P14 $CD8^+$ T cells (provided by Dr. Rafi Ahmed, Emory University, School of Medicine, Atlanta, GA, USA) were isolated from the spleens of wild-type P14 mice and labeled with 2.5 μM Cell Trace Violet (CTV) (Life Technologies) for 30 min at 37 °C and washed with RPMI containing 10 % FBS. A total of 5×10^4 labeled T cells were cocultured in RPMI containing 10 % FBS with 1×10^4 BMDCs or BMDCs treated with 0-, 1-, 2-, and 3-year-aged PP microplastics. After 72 h, the cells were harvested, stained, and analyzed by flow cytometry. The colocalization of BMDCs and T cells was evaluated by confocal microscopy (Carl Zeiss). After 72 h of coculture of DiD-stained BMDCs and P14 $CD8^+$ T cells, unbound BMDCs were removed by centrifugation at 2,500 rpm for 2 min. The P14 $CD8^+$ T cells were stained with DAPI (Sigma Aldrich) and FITC-labeled anti-CD8 (BD Biosciences) for 45 min after blocking for visualization.

4.8. A549 and NCI-H1650 cell culture and in vitro evaluation of cell proliferation

Human non-small cell lung cancer cell lines (NCI-H1650, A549) were obtained from the Korean Cell Line Bank (Seoul, Korea). Both cell lines were cultured in RPMI 1640 (# 22400071, Gibco) supplemented with 10 % heat-inactivated fetal bovine serum (#S001-01, Welgene, Gyeongsan, Korea) and 1 % penicillin–streptomycin-glutamine (#10378016, Gibco), which is referred to as the growth medium below. The morphology of A549 and NCI-H1650 cells was observed by microscopy. To investigate the proliferation in response to the samples, 15 000 cells per well were seeded in 12 well plates and 0-, 1-, 2-, and 3-year-aged PP microplastics were simultaneously loaded at concentrations of 100, 10, 1, 0.5 and 0.1 μg/mL (n = 3). After 1 day of treatment, cells were washed with PBS, and a cell counting kit-8 (CCK-8) reagent (#CCK-3000, Dongin Biotech Co., Korea) was added to the culture medium, followed by a 1 h incubation. The absorbance at a wavelength of 450 nm was detected using a plate reader (Spectra Max 340 PC; Molecular Devices, San Jose, CA, USA). Cells were then thoroughly washed by PBS to eliminate the CCK-8 reagents, then subsequently treated with the same volume of growth medium containing the same concentration of PP microplastics on the first day. After another 2 days of culture, we repeated the same process to evaluate the proliferation on day 3. The process described above was repeated every 2 days until day 7 (1 week).

4.9. Proliferation, drug resistance, metastasis trafficking

A549 and NCI-H1650 cells (1×10^5 cells) were added into individual wells of a 6-well plates and treated with 100 μg/mL of 0-, 1-, 2-, and 3-

year aged PP microplastics for 7 days. Cells was washed with PBS during culture. On day 7, flow cytometry analysis was conducted to compare the proliferation and drug resistance using Ki-67 marker, as well as elongation and metastasis using the Notch-1 marker. Briefly, the cells were fixed with PBS containing 4 % paraformaldehyde for 20 min at room temperature and then washed twice in permeabilization buffer (PBS containing 1 % FBS, 0.3 % saponin, and 0.1 % Na azide). Next, the cells were incubated for 1 h with anti-Notch-1 (#12–5785-82, PE, eBioscience) and anti-Ki-67 (#53-5698-82, Alexa Fluor™ 488, eBioscience). The cells were then washed with permeabilization buffer three times. Finally, the 7-AAD staining solution was added and incubated for 30 min. The data were acquired using a BD FACSVerse system (BD Bioscience, CA, USA) and analyzed with FlowJo X software (Flowjo, LLC, Ashland, OR, USA). To additionally check the drug resistance of aged PP microplastics, A549 and NCI-H1650 cells (1×10^5 cells) were seeded with PP microplastics in 12 well plate (n = 3) and treated with 50 μg/mL of cisplatin for 2 days. Cells were then treated with CCK-8 assay reagents to determine the cell viability.

4.10. Proliferation, drug resistance, and metastasis trafficking

A549 and NCI-H1650 cells (1×10^5 cells) in 6 well plates were incubated with PP microplastics for intracellular ROS estimation. Non-adherent cells were centrifuged to collect the supernatant and the cells were processed directly for intracellular reactive oxygen species (ROS) estimation. Adherent cells were washed with PBS and dissociated from the plate using Trypsin-EDTA(0.25 %), phenol red (#25200058, Gibco). The cells were collected in 1 mL microtubes and further washed twice with PBS. The DCF-DA staining assay was employed to measure intracellular ROS production. 2′,7′ −dichlorodihydrofluorescein diacetate (H2DCF-DA) is a non-fluorescent compound that transforms into DCF, a fluorescent derivative, in the presence of ROS. 20 μM H2DCF-DA (Sigma) was added to each tube and incubated at 37 °C for 45 min. After a single PBS wash, data acquisition was performed using a BD FACSVerse system (BD Bioscience, CA, USA). Finally, the acquired data was analyzed with FlowJo X software (Flowjo, LLC, Ashland, OR, USA).

4.11. Quantification of polypropylene microplastics during the washing of cells

To quantify the washed PP microplastics during 7 days of culture, PP microplastics were stained by Nile red (Sigma) with the ratio of 10:1. 15 000 A549 cells per well were seeded in 12 well plates and 0-, 1-, 2-, and 3-year-aged Nile red-stained PP microplastics were simultaneously loaded at concentrations of 100 μg/mL. After 1 day of treatment, the supernatant of cells was collected. PBS were added to the cells for washing, and the supernatant was collected again. The Nile red-stained PP microplastics in the collected supernatant were measured by UV–vis spectrometer (Evolution 300, Thermo Fisher, CA, USA).

4.12. Quantification and statistical analysis

Statistical analysis was performed using Origin 2018 software. Comparisons between multiple groups were performed using one-way ANOVA with Tukey's post hoc test. Statistical details, including the statistical test, n value, precision measure, and statistical significance, are reported in the figures and figure legends. Each graph in the figure set shows the mean ± SEM. Data are representative at least two independent experiments (n = 3/group). *P < 0.05; **P < 0.01; ***P < 0.001; ****P < 0.0001.

CRediT authorship contribution statement

Yoojin Lee: Writing – original draft, Methodology, Conceptualization. **Sung-eun Heo:** Visualization, Methodology, Investigation. **Kyungtae Park:** Visualization, Validation, Investigation. **Hyungseok Yong:** Writing – review & editing, Validation, Data curation. **Yongho Lee:** Methodology. **Taihyun Kim:** Visualization. **Yoonsung Noh:** Methodology, Validation. **Woojin Choi:** Writing – review & editing. **Bumgyu Choi:** Methodology, Visualization. **Dahae Kim:** Methodology. **Chae-Won Moon:** Methodology. **Sang-Jun Ha:** Writing – review & editing, Methodology. **Jinkee Hong:** Supervision, Project administration.

Declaration of competing interest

The authors declare that they have no known competing financial interests or personal relationships that could have appeared to influence the work reported in this paper.

Acknowledgements

This work was supported by the National Research Foundation of Korea (NRF) grant funded by the Korea government (MSIT)(RS-2024-00354178). This research was also supported by a grant of the Korea-US Collaborative Research Fund (KUCRF), funded by the Ministry of Science and ICT and Ministry of Health & Welfare, Republic of Korea (grant number: RS-2024-00468036).

Appendix A. Supplementary data

Supplementary data to this article can be found online at https://doi.org/10.1016/j.cej.2025.163302.

Data availability

The data that has been used is confidential.

References

[1] D.T. Field, J.L. Green, R. Bennett, L.C. Jenner, R. Laura, E.C. Sadofsky, M. Loubani, J.M. Rotchell, Microplastics in the surgical environment, Environ. Int. 170 (2022) 107630, https://doi.org/10.1016/j.envint.2022.107630.
[2] J.H. Park, S. Hong, O.-H. Kim, C.-H. Kim, J. Kim, J.-W. Kim, S. Hong, H.J. Lee, Polypropylene microplastics promote metastatic features in human breast cancer, Sci. Rep. 13 (2023) 6252, https://doi.org/10.1038/s41598-023-33393-8.
[3] H. Kim, J. Zaheer, E.-J. Choi, J.S. Kim, Enhanced ASGR2 by microplastic exposure leads to resistance to therapy in gastric cancer, Theranostics 12 (7) (2022) 3217–3236, https://doi.org/10.7150/thno.73226.
[4] Y. Wang, Xu. Xinqi, G. Jiang, Microplastics exposure promotes the proliferation of skin cancer cells but inhibits the growth of normal skin cells by regulating the inflammatory process, Ecotoxicol. Environ. Saf. 267 (2023) 115636, https://doi.org/10.1016/j.ecoenv.2023.115636.
[5] W. Pengfei, S. Lin, G. Cao, W. Jiabin, H. Jin, C. Wang, M.H. Wong, Z. Yang, Z. Cai, Absorption, distribution, metabolism, excretion and toxicity of microplastics in the human body and health implications, J. Hazardous Mater. 437 (2022) 129361, https://doi.org/10.1016/j.jhazmat.2022.129361.
[6] L.F. Amato-Lourenço, R. Carvalho-Oliveira, G.R. Júnior, L. dos Santos, R.A. Galvão, T.M. Ando, T. Mauad, Presence of airborne microplastics in human lung tissue, J. Hazard. Mater. 416 (2021) 126124, https://doi.org/10.1016/j.jhazmat.2021.126124.
[7] L.C. Jenner, J.M. Rotchell, R.T. Bennett, M. Cowen, V. Tentzeris, L.R. Sadofsky, Detection of microplastics in human lung tissue using μFTIR spectroscopy, Sci. Total Environ. 831 (2022) 154907, https://doi.org/10.1016/j.scitotenv.2022.154907.
[8] T. Kim, K. Park, J. Hong, Understanding the hazards induced by microplastics in different environmental conditions, J. Hazardous Mater. 424 (2022) 127630, https://doi.org/10.1016/j.jhazmat.2021.127630. Part C.
[9] M. Dong, Q. Zhang, X. Xing, W. Chen, Z. She, Z. Luo, Raman spectra and surface changes of microplastics weathered under natural environments, Sci. Total Environ. 739 (2020) 139990, https://doi.org/10.1016/j.scitotenv.2020.139990.
[10] M.A. Beard, O.R. Ghita, K.E. Evans, Using Raman spectroscopy to monitor surface finish and roughness of components manufactured by selective laser sintering, J. Raman Spectrosc. 42 (4) (2011) 744–748, https://doi.org/10.1002/jrs.2771.
[11] S.-U. Fang, C.-L. Hsu, T.-C. Hsu, M.-Y. Juang, Y.-C. Liu, Surface roughness-correlated SERS effect on Au island-deposited substrate, J. Electroanal. Chem. 741 (2015) 127–133, https://doi.org/10.1016/j.jelechem.2015.01.028.
[12] L. Mikoliunaite, R.D. Rodriguez, E. Sheremet, V. Kolchuzhin, J. Mehner, A. Ramanavicius, D.R.T. Zahn, The substrate matters in the Raman spectroscopy analysis of cells, Sci. Rep. 5 (2015) 13150, https://doi.org/10.1038/srep13150.
[13] A.K. Chaudhary, K. Chaitanya, R.P. Vijayakumar, Synergistic effect of UV and chemical treatment on biological degradation of Polystyrene by Cephalosporium

strain NCIM 1251, Arch. Microbiol. 203 (2021) 2183–2191, https://doi.org/10.1007/s00203-021-02228-3.
[14] S. Ali, Z. Khatri, O. Kyung Wha, I.-S. Kim, S.H. Kim, Zein/cellulose acetate hybrid nanofibers: Electrospinning and characterization, Macromol. Res. 22 (2014) 971–977, https://doi.org/10.1007/s13233-014-2136-4.
[15] T.-B.-C. Ho, T.B. Nguyen, C.P. Chiu-Wen Chen, W.-H.C. Huang, S. Hsieh, P.-T. Nguyen, Cheng-Di Dong, Influence of aging processes on PE microplastics with various oxidants: Morphology, chemical structure, and adsorption behavior toward tetracycline, Environ. Technol. Innov. 31 (2023) 103173, https://doi.org/10.1016/j.eti.2023.103173.
[16] R. Hughes, B.-Z. Qian, C. Rowan, M. Muthana, I. Keklikoglou, C.O. Olson, S. Tazzyman, S. Danson, C. Addison, M. Clemons, A.M. Gonzalez-Angulo, J. A. Joyce, M. De Palma, J.W. Pollard, C.E. Lewis, Perivascular M2 macrophages stimulate tumor relapse after chemotherapy, Cancer research 763 (2016) 6828–6838, https://doi.org/10.1158/0008-5472.CAN-16-1114.
[17] L. Zhao, W. Shi, Hu. Fangfang, X. Song, Z. Cheng, J. Zhou, Prolonged oral ingestion of microplastics induced inflammation in the liver tissues of C57BL/6J mice through polarization of macrophages and increased infiltration of natural killer cells, Ecotoxicol. Environ. Saf. 227 (2021) 112882, https://doi.org/10.1016/j.ecoenv.2021.112882.
[18] W. Kwon, D. Kim, H.-Y. Kim, S.W. Jeong, S.-G. Lee, H.-C. Kim, Y.-J. Lee, M. K. Kwon, J.-S. Hwang, J.E. Hanc, J.K. Park, S.-J. Lee, S.-K. Choi, Microglial phagocytosis of polystyrene microplastics results in immune alteration and apoptosis in vitro and in vivo, Sci. Total Environ. 807 (2022) 150817, https://doi.org/10.1016/j.scitotenv.2021.150817.
[19] S. Li, L. Liu, Yu. Gang Luo, D.H. Yuan, F. Xiao, The crosstalk between M1 macrophage polarization and energy metabolism disorder contributes to polystyrene nanoplastics-triggered testicular inflammation, Food Chem. Toxicol. 180 (2023) 114002, https://doi.org/10.1016/j.fct.2023.114002.
[20] S. Hamlet, M. Alfarsi, R. George, S. Ivanovski, The effect of hydrophilic titanium surface modification on macrophage inflammatory cytokine gene expression, Clin. Oral Implant Res. 23 (5) (2012) 584–590, https://doi.org/10.1111/j.1600-0501.2011.02325.x.
[21] J. Li, Y.-J. Zhang, Z.-Y. Lv, K. Liu, C.-X. Meng, B.o. Zou, K.-Y. Li, F.-Z. Liu, B. Zhang, The observed difference of macrophage phenotype on different surface roughness of mineralized collagen, Regener. Biomater. 7 (2) (2020) 203–211, https://doi.org/10.1093/rb/rbz053.
[22] Y. Li, L.e. Tao, Q. Wang, F. Wang, G. Li, M. Song, Potential health impact of microplastics: a review of environmental distribution human exposure, and toxic effects, Environ. Health 1 (4) (2023) 249–257, https://doi.org/10.1021/envhealth.3c00052.
[23] Y. Lee, S. Cho, K. Park, T. Kim, J. Kim, D.-Y. Ryu, J. Hong, Potential lifetime effects caused by cellular uptake of nanoplastics: A review, Environ. Pollut. 329 (2023) 121668, https://doi.org/10.1016/j.envpol.2023.121668.
[24] K. Mrouj, N. Andrés-Sánchez, G. Dubra, D. Fisher, Ki-67 regulates global gene expression and promotes sequential stages of carcinogenesis, Procee. Nat. Academy. Sci. (PNAS) 118 (10) (2021) e2026507118, https://doi.org/10.1073/pnas.2026507118.
[25] S.M. Lyons, E. Alizadeh, J. Mannheimer, K. Schuamberg, J. Castle, B. Schroder, P. Turk, D. Thamm, A. Prasad, Changes in cell shape are correlated with metastatic potential in murine and human osteosarcomas, Bio. Open 5 (2016) 289–299, https://doi.org/10.1242/bio.013409.
[26] V. Gensbittel, M. Krater, S. Harlepp, I. Busnelli, J. Guck, J.G. Goetz, Mechanical adaptability of tumor cells in metastasis, Develop. Cell 56 (2) (2021) 164–179, https://doi.org/10.1016/j.devcel.2020.10.011.
[27] K. Miyazaki, J. Oyanagi, D. Hoshino, S. Togo, H. Kumagai, Y. Miyagi, Cancer cell migration on elongate protrusions of fibroblasts in collagen matrix, Sci. Rep. 9 (2019) 292, https://doi.org/10.1038/s41598-018-36646-z.
[28] S. Saha, J.V. Hof, Cotton fiber cells are arrested at G1 stage, J. New Seeds 7 (1) (2005) 1–8, https://doi.org/10.1300/J153v07n01_01.
[29] Y.H. Han, W.H. Park, MG132 as a proteasome inhibitorinduces cell growth inhibition and celldeath in A549 lung cancer cells viainfluencing reactive oxygen speciesand GSH level, Hum. Exp. Toxicol. 29 (7) (2010) 607–614, https://doi.org/10.1177/0960327109358733.
[30] M. Segovia-Mendoza, K.E. Nava-Castro, M.I. Palacios-Arreola, C. Garay-Canales, J. Morales-Montor, How microplastic components influence the immune system and impact on children health: Focus on cancer, Birth Defects Res. 112 (17) (2020) 1341–1361, https://doi.org/10.1002/bdr2.1779.
[31] H. Jeong, W. Kim, D. Choi, J. Heo, U. Han, S.Y. Jung, H.H. Park, S.-T. Hong, J. H. Park, J. Hong, Potential threats of nanoplastic accumulation in human induced pluripotent stem cells, Chem. Eng. J. 427 (2022) 131841, https://doi.org/10.1016/j.cej.2021.131841.
[32] J. Hwang, D. Choi, S. Han, J. Choi, J. Hong, An assessment of the toxicity of polypropylene microplastics in human derived cells, Sci. Total Environ. 684 (2019) 657–669, https://doi.org/10.1016/j.scitotenv.2019.05.071.
[33] W. Cheng, H. Chen, Y. Zhou, Y. You, D. Lei, Y. Li, Y. Feng, Y. Wang, Aged fragmented-polypropylene microplastics induced ageing statues-dependent bioenergetic imbalance and reductive stress: In vivo and liver organoids-based in vitro study, Environ. Int. 191 (2024) 108949, https://doi.org/10.1016/j.envint.2024.108949.
[34] P. Aubrecht, P. Malinský, J. Novák, J. Smejkal, A. Jagerová, J. Matoušek, M. Štofik, M. Liegertová, J. Luxa, A. Macková, J. Malý, Patterning of COC polymers by middle-energy ion beams for selective cell adhesion in microfluidic devices, Adv. Mater. Interfaces 11 (18) (2024) 2301077, https://doi.org/10.1002/admi.202301077.
[35] B. Majhya, P. Priyadarshinia, A.K. Sen, Effect of surface energy and roughness on cell adhesion and growth – facile surface modification for enhanced cell culture, RSC Adv. 11 (2021) 15467–15476, https://doi.org/10.1039/D1RA02402G.
[36] X. Qiu, S. Ma, J. Zhang, L. Fang, X. Guo, L. Zhu, Dissolved organic matter promotes the aging process of polystyrene microplastics under dark and ultraviolet light conditions: the crucial role of reactive oxygen species, Environ. Sci. Tech. 56 (14) (2022) 10149–10160, https://doi.org/10.1021/acs.est.2c03309.
[37] H. Wang, P. Liu, M. Wang, Wu. Xiaowei, Y. Shi, H. Huang, S. Gao, Enhanced phototransformation of atorvastatin by polystyrene microplastics: Critical role of aging, J. Hazard. Mater. 408 (2021) 124756, https://doi.org/10.1016/j.jhazmat.2020.124756.
[38] B. Majhya, P. Priyadarshinia, A.K. Sen, Effect of surface energy and roughness on cell adhesion and growth – facile surface modification for enhanced cell culture, RSC Adv. 11 (25) (2021) 15467–15476, https://doi.org/10.1039/d1ra02402g.
[39] M. Wang, Yu. Fei, Y. Zhang, P. Li, Novel insights into Notch signaling in tumor immunity: potential targets for cancer immunotherapy, Front. Immunol. 15 (2024) 1352484, https://doi.org/10.3389/fimmu.2024.1352484.
[40] A. Kim, E.Y. Kim, E.N. Cho, H.J. Kim, S.K. Kim, J. Chang, C.M. Ahn, Y.S. Chang, Notch1 destabilizes the adherens junction complex through upregulation of the Snail family of E-cadherin repressors in non-small cell lung cancer, Oncol. Rep. 30 (3) (2013) 1423–1429, https://doi.org/10.3892/or.2013.2565.
[41] M.G. Scioli, S. Terriaca, E. Fiorelli, G. Storti, G. Fabbri, V. Cervelli, A. Orlandi, Extracellular vesicles and cancer stem cells in tumor progression: new therapeutic perspectives, Int. J. Mol. Sci. 22 (19) (2021) 10572, https://doi.org/10.3390/ijms221910572.
[42] K. Mierzejewski, A. Kurzyńska, M. Golubska, J. Całka, I. Gałęcka, M. Szabelski, Ł. Paukszto, A. Andronowska, I. Bogacka, New insights into the potential effects of PET microplastics on organisms via extracellular vesicle-mediated communication, Sci. Total Environ. 904 (2023) 166967, https://doi.org/10.1016/j.scitotenv.2023.166967.
[43] J. Järvenpää, M. Rahnasto-Rilla, M. Lahtela-Kakkonen, J. Küblbeck, Profiling the regulatory interplay of BET bromodomains and Sirtuins in cancer cell lines, Biomed. Pharmacother. 147 (2022) 112652, https://doi.org/10.1016/j.biopha.2022.112652.
[44] T. Anwar, S. Khosla, G. Ramakrishna, Increased expression of SIRT2 is a novel marker of cellular senescence and is dependent on wild type p53 status, Cell Cycle 15 (14) (2016) 1883–1897, https://doi.org/10.1080/15384101.2016.1189041.
[45] Y. Zhang, X. Cheng, J.A. Jansen, F. Yang, J.J.P. van den Jeroen, Beucken,, Titanium surface characteristics modulate macrophage polarization, Mater. Sci. Eng.: C 95 (2019) 143–151, https://doi.org/10.1016/j.msec.2018.10.065.
[46] W. He, S.i. Liu, W. Zhang, K. Yi, C. Zhang, H. Pang, D.H.J. Huang, X. Li, Recent advances on microplastic aging: Identification, mechanism, influence factors, and additives release, Sci. Total Environ. 889 (2023) 164035, https://doi.org/10.1016/j.scitotenv.2023.164035.
[47] Xu. Zhe, J. Zhang, R. Qi, Q.i. Liu, H. Cao, F. Wen, Y. Liao, K. Shih, Y. Tang, Complex release dynamics of microplastic additives: An interplay of additive degradation and microplastic aging, J. Hazard. Mater. 490 (2025) 137711, https://doi.org/10.1016/j.jhazmat.2025.137711.
[48] P. Liu, Y. Shi, Wu. Xiaowei, H. Wang, H. Huang, X. Guo, S. Gao, Review of the artificially-accelerated aging technology and ecological risk of microplastics, Sci. Total Environ. 768 (2021) 144969, https://doi.org/10.1016/j.scitotenv.2021.144969.
[49] Standard Guide for Accelerated Aging of Sterile Barrier Systems for Medical Devices, ASTM International (2007).